Top quark and Higgs boson masses from wormhole physics

B. A. Harris* and G. C. Joshi†

School of Physics, University of Melbourne, Parkville, Victoria 3052, Australia

(Received 28 April 1994)

We bring together quantum field theory on S_4 with the Coleman wormhole hypothesis, which imposes constraints on terms in the gravitational Lagrangian. In particular, we investigate the effect of matter fields on the trace anomaly, which is related to the (curvature)^2 terms, by the use of the renormalization group equations. We consider a toy model of a nonconformally coupled Higgs boson to a single "top" quark. By numerically solving the renormalization group equations for the couplings of the model, we can find preferred values of the particle masses for various values of the bare nonconformal coupling. By making the *ad hoc* assumption that the tree-level, Higgs boson trace anomaly vanishes on shell, a unique prediction can be made within this model for the masses of both the Higgs boson and the top quark.

PACS number(s): 11.10.Hi, 04.60.−m, 14.65.Ha, 14.80.Bn

I. INTRODUCTION

Recently, it was suggested [1] by Coleman that the effect of wormholes in Euclidean quantum gravity is to modify or even determine the observed values of the fundamental constants. In this idea, the effects of wormholes can be described by a set of parameters $\{\alpha_i\}$. The cosmological constant Λ, the gravitational constant G, and other matter couplings depend on $\{\alpha_i\}$, in a complicated way, at the wormhole scale which is around or just below the Planck scale. Furthermore, Coleman suggested a mechanism by which Λ is exactly zero and G assumes its minimum possible value. In the Euclidean functional integral, it is possible [2] to integrate out the contribution of wormhole configurations to give an integral over a distribution of parameters. It is suggested that the dominant contribution comes from classical saddle points of the integral. The distribution is of the form

$$Q(\alpha) = e^{e^{-\Gamma_{\text{eff}}\{\alpha_i\}}} . \tag{1}$$

For the action

$$\Gamma[g] = \int d^4x \left[\Lambda - \frac{R}{16\pi G} + aR_{\mu\nu\sigma\lambda}R^{\mu\nu\sigma\lambda} \right.$$
$$\left. +bR_{\mu\nu}R^{\mu\nu} + cR^2 \right] , \tag{2}$$

with $\Lambda > 0$, the stationary point is a four-sphere of radius

$$a = \left(\frac{3}{8G\Lambda} \right)^{1/2} , \tag{3}$$

with

$$\Gamma_{\text{eff}} = -\frac{3}{8G^2\Lambda} + \frac{8\pi^2 d}{3} , \tag{4}$$

where d is a linear combination of a, b, and c. The double exponential makes the $\Lambda=0$ surface in α space overwhelmingly likely, and the minimization of G and d on that surface should fix some or all of the other constants of nature. Since the higher-derivative terms are related to the trace anomaly [3], there have been attempts [4,5] to use renormalization group techniques to relate the coupling constants of interacting field theories to the constant d. The tendency for Λ to vanish means that one is forced to compute the effective action in the limit of large radius, that is, in the far infrared limit, where all but massless particles have been integrated out.

In this paper, we apply the renormalization group to look at how minimizing d affects the masses of the Higgs boson and the top quark. In Sec. II, we give a brief outline of how the minimization of d can determine particle masses. In Sec. III, we present a toy model with a Higgs scalar and a single top quark. We carry out the one-loop renormalization of the model to derive the renormalization group equations for the couplings of the model. We then calculate the vacuum diagrams to two-loop order to derive the corresponding equation for the parameter d. These equations are then solved numerically, and regions in coupling constant space are sought which minimize d at low energies.

II. RENORMALIZATION GROUP ANALYSIS

In Refs. [3,6–8], quantum corrections to the constant d were calculated. These give rise to a renormalization group equation which describes how d changes as the quantum fluctuations are integrated out going from a high-mass scale down to a low-mass scale. Defining $D \equiv 8\pi^2 d/3$, we have an equation of the form

$$\mu \frac{\partial D}{\partial \mu} = -A_1 + \gamma(g_i) , \tag{5}$$

---

*Electronic address: bah@tauon.ph.unimelb.edu.au
†Electronic address: joshi@tauon.ph.unimelb.edu.au

where A_1 is the one-loop free field contribution and $\gamma(g_i)$ is the β function obtained from higher-order interactions. Given that wormholes are unable to dictate the particle content of the world, which presumably arises from some superstring theory or the like, the wormholes will attempt to minimize D at large distances, that is, in the infrared limit, by adjusting the fundamental couplings at the wormhole scale.

Putting aside the interacting part for the moment, one can solve Eq. (5) to obtain

$$D(\mu) = D(M_{\text{wh}}) + \sum A_{1i} \ln(M_{\text{wh}}/\mu) \ . \tag{6}$$

This equation holds as one runs down from the wormhole scale until the mass scale associated with each particular field is reached. At this point, the field is integrated out and stops contributing. In the standard model, the only fields left in the massless limit are the photon and graviton. Since wormholes will try to minimize D, the sign of A_1 is important. Referring to Eq. (40) of Ref. [7],

$$A_1 = -\tfrac{62}{180}N_{\text{GB}} - \tfrac{11}{180}N_f - \tfrac{2}{180}N_b \ , \tag{7}$$

we have $A_1 > 0$ for gauge bosons, fermions, and conformal scalar fields. Although the values were calculated for massless fields, dimensional analysis requires that the results hold for massive fermions and scalars as well, since masses will only contribute to Λ and G. However, for nonconformally coupled scalars, the sign of A_1 may change [4]. An investigation for spin-$\tfrac{3}{2}$ and massive vector particles is given in Ref. [9]. For a field with $A_1 > 0$, $D(\mu)$ will increase with decreasing μ. This leads to the conclusion that if the field has an adjustable bare mass at the wormhole scale, then this mass will be driven up to that scale in order to minimize the contribution to D. This problem may be evaded provided there is a symmetry such as gauge invariance for vector bosons or exact chiral symmetry for fermions. Any physical mass will then have to be induced through a process such as spontaneous symmetry breaking. For a conformal scalar, there is no such protection and one is forced to consider that scalars may require a nonconformal coupling of the form suggested in Ref. [4]. We investigate this possibility in the next section.

Another conclusion which may be drawn is that if we have a model with a Higgs field, then the wormhole parameters will adjust the couplings to raise the symmetry-breaking scale to eliminate the gauge bosons and fermions as quickly as possible. However, this is barely more than a restatement of the hierarchy problem in a different context.

III. TOP QUARK AND HIGGS BOSON MASSES

In this section, we investigate the possible effect of wormholes on the values of the top quark and Higgs boson masses. There have been attempts to address these questions separately [4,5], but because of the strong influence on the Higgs boson mass by the top quark Yukawa coupling, it would appear to be necessary to look at both

together. The interdependence of the Higgs boson and top quark masses has been investigated previously by a variety of authors [10–15] and collected in a review by Sher [16]. The various results will be useful in what follows.

We choose a simple model containing a single neutral "Higgs" boson coupled to a Dirac "top" quark. The quark is coupled to SU(3), and we assume that the other quarks in the standard model contribute to the running of the QCD coupling constant. The scalar field has a quartic self-coupling as well as a nonminimal coupling to the gravitational field. The importance of this nonminimal coupling will become clear shortly.

We are neglecting here the effect of the electroweak couplings since they only have a large effect on the Higgs boson mass for small values of the top Yukawa coupling. This implies that this model will only be useful provided the bound $4m_t^4 > 2M_W^4 + m_Z^4$, given in Ref. [12], is satisfied, which at the tree level gives $m_t > 77$ GeV. Given the current experimental fits to the top mass, for example, del Aguila, Martinez, and Quiros [17] with $m_t = 122^{+25}_{-20}$ GeV, this would appear to be a reasonable assumption.

The action for the model is

$$
\begin{aligned}
I = \int d\sigma \Bigg[& \frac{1}{2} Z_\phi \phi \left(-M + \frac{1}{a^2}\zeta \right) \phi \\
& + \frac{1}{2a^2} Z_\phi \delta\zeta\phi^2 + \frac{\lambda}{4!} Z_\lambda \phi^4 + Z_2 \bar\psi\gamma^a \left(D_a - \frac{n}{2a^2}\eta_a \right) \psi \\
& - g Z_1 \bar\psi\gamma^a Q_{ab} A_A^b T^A \psi + \frac{g_t}{\sqrt{2}} Z_{g_t} \phi\bar\psi\psi \Bigg] \ ,
\end{aligned} \tag{8}
$$

where the counterterms and wave function renormalizations have been included. The Feynman rules for this model are given in the Appendix. Of course, there is also the non-Abelian sector as well as the other quarks which we have omitted.

The major difference between this model and those of previous papers [7,8] is the nonminimal coupling of the scalar field. This has the effect of modifying the scalar propagator

$$
\begin{aligned}
G_\zeta(\eta,\eta') &= \left[-M + \frac{1}{a^2}\zeta \right]^{-1} (\eta,\eta') \\
&= a^2 \sum_{l=0}^{\infty} G_\zeta(l) Y_{lm}(\eta) Y_l^{*m}(\eta') \ ,
\end{aligned} \tag{9}
$$

where

$$G_\zeta(l) = \frac{1}{[l + \tfrac{1}{2}(n-1) + Y][l + \tfrac{1}{2}(n-1) - Y]} \tag{10}$$

and

$$Y = \sqrt{\tfrac{1}{4} - \zeta^2} \ . \tag{11}$$

That this modification has little effect on the complexity of the calculations is another example of the power of the complex l-plane technique. The sums are evaluated in the same way, with the dependence of the propagator poles on ζ being the only difference.

A. One-loop renormalization

The one-loop renormalization of this model is carried out in a straightforward way using the techniques of Ref. [7]. The diagrams are given in Fig. 1. The ζ counterterm and the relevant renormalization constants are found to be

$$Z_{g_t} = 1 - \frac{1}{16\pi^2}(4g^2 C_f - \tfrac{1}{2}g_t^2)\left(\frac{2}{\varepsilon}\right) , \qquad (12)$$

$$Z_2 = 1 - \frac{1}{16\pi^2}(g^2 C_f + \tfrac{1}{4}g_t^2)\left(\frac{2}{\varepsilon}\right) , \qquad (13)$$

$$Z_\phi = 1 - \frac{1}{16\pi^2}g_t^2 N_f \left(\frac{2}{\varepsilon}\right) , \qquad (14)$$

$$\delta\zeta = \frac{\zeta}{16\pi^2}(g_t^2 N_f + \tfrac{1}{2}\lambda)\left(\frac{2}{\varepsilon}\right) , \qquad (15)$$

$$Z_\lambda = 1 - \frac{1}{16\pi^2}\left(\frac{6}{\lambda}g_t^4 N_f - \frac{3}{2}\lambda\right)\left(\frac{2}{\varepsilon}\right) , \qquad (16)$$

where we have kept the non-Abelian Casimir invariants general, using the conventions of Ref. [18].

B. Vacuum diagrams

Now as we have seen in Ref. [7], vacuum diagrams also require a renormalization of the gravitational part of the action. To one loop we have the diagrams of Fig. 2. For the fermion we have, from Refs. [6,7],

$$\Gamma_f^1[0] = \tfrac{11}{180}N_f \left(\frac{2}{\varepsilon}\right) + O(\varepsilon^0) , \qquad (17)$$

but for the nonconformal scalar the procedure is slightly modified as a result of the presence of the coupling ζ. We have

$$\Gamma_S^1[0] = -\ln\left\{ \det\left[-\frac{1}{\mu^2}\left(-M + \frac{1}{a^2}\zeta \right) \right]^{-1/2} \right\}$$

$$= \tfrac{1}{2}\sum_{l=0}^{\infty} \ln\left[\frac{1}{\mu^2 a^2}[l + \tfrac{1}{2}(n-1) - Y][l + \tfrac{1}{2}(n-1) + Y] \right] \dim(l,0)$$

$$= \frac{1}{\Gamma(n)\sin\pi(n/2 - 2)}\{I_1(n) + I_2(n)\} , \qquad (18)$$

where

$$I_1(n) = -\int_{-(1/2-Y)}^{0} dx\, \sin\pi x \left(x + \frac{1}{2} \right) \Gamma\left(\frac{n}{2} + x \right)$$
$$\times \Gamma\left(\frac{n}{2} - 1 - x \right) \qquad (19)$$

and

$$I_2(n) = -\operatorname{Im}\left\{ i \int_0^{\infty} dy\, e^{-\pi y} \left(\frac{1}{2} + iy \right) \Gamma\left(\frac{n}{2} + iy \right) \right.$$
$$\left. \times \Gamma\left(\frac{n}{2} - 1 - iy \right) \right\} . \qquad (20)$$

Z_{gt}

Z_2
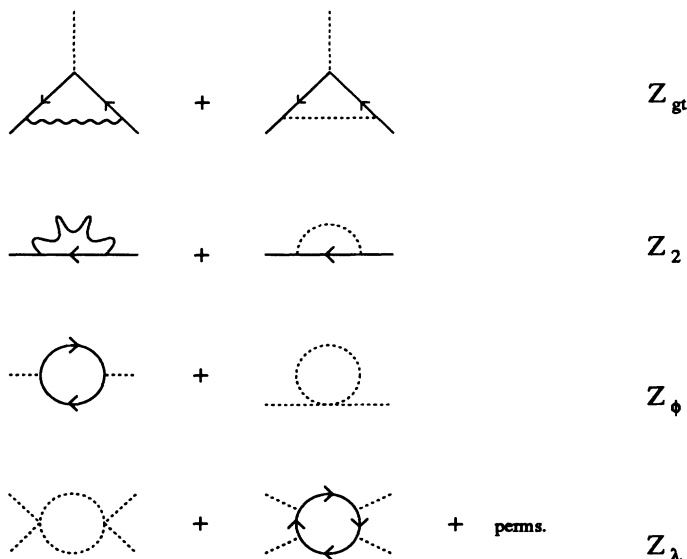
Z_ϕ , $\delta\zeta$

Z_λ

FIG. 1. One-loop field renormalization diagrams.

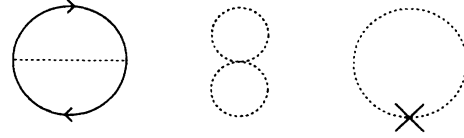FIG. 2. One-loop vacuum diagrams.

FIG. 3. Two-loop vacuum diagrams.

Note that $I_2(n)$ is the contribution from the conformal part of the propagator and is half of the result from Ref. [7], since we are dealing with a neutral field. Evaluating the integrals at $n = 4$, we obtain

$$\Gamma^1_S[0] = (\tfrac{1}{180} - \tfrac{1}{24}\zeta^2)\left(\frac{2}{\varepsilon}\right) . \tag{21}$$

This result agrees with Ref. [4] and also the last chapter of Ref. [19] once normalization differences are accounted for. We therefore require the counterterm

$$I_{ct} = \int d\sigma \, \mu^{-\varepsilon} \frac{1}{a^4 \Omega_5} \{ -\tfrac{11}{180} N_f + (\tfrac{1}{24}\zeta^2 - \tfrac{1}{180}) \} \left(\frac{2}{\varepsilon}\right) . \tag{22}$$

We now turn to the interacting two-loop vacuum diagrams given in Fig. 3. The techniques to handle such diagrams have been described in Ref. [7]. In the following, we adopt the slightly different convention $\mathrm{TR}(I)=4$ for the Γ matrices than that used in Ref. [20], $\mathrm{TR}(I) = 2^{n/2}$, to eliminate an annoying prescription dependence which feeds through to the two-loop renormalization group equations. The change in convention simply results in a finite renormalization of the $\delta\zeta$ counterterm and the vertex constant Z_{g_t}.

For the scalar-fermion loop, we have

$$\Gamma^2_{Sf}[0] = -\frac{g_t^2 N_f}{\Gamma(n)\Omega_{n+1}}(\mu a)^{4-n} \frac{1}{2(n-1)\Gamma^2[\frac{1}{2}(n-1)]} \sum_{l=0}^{\infty}\sum_{s=0}^{\infty}\sum_{J=0}^{\infty} \tilde{G}(l)\tilde{G}(s)\tilde{G}_\zeta(J)A(l,s,J)F(l,s,J) , \tag{23}$$

where $A(l,s,J)$ is given by

$$A(l,s,J) = \left\{ \left(\frac{n}{2}-1\right)^2 + \tfrac{1}{2}[-J(J+n-1) + l(l+n-1) + s(s+n-1)] \right\} . \tag{24}$$

Evaluating the l and s sums gives

$$\Gamma^2_{Sf}[0] = \frac{g_t^2 N_f}{\Gamma(n)\Omega_{n+1}}(\mu a)^{4-n} \frac{2^{6-2n}\pi}{2(n-1)\Gamma^2[\frac{1}{2}(n-1)]} \frac{\pi}{\sin\pi(n/2-2)} \sum_{J=0}^{\infty} \tilde{G}_\zeta(J)A\left(-\frac{n}{2},-\frac{n}{2},J\right)\frac{\Gamma[J+n-1]\Gamma[J+n-2]}{\Gamma[J+2]\Gamma[J+1]}$$

$$= \frac{g_t^2 N_f}{\Gamma(n)\Omega_{n+1}}(\mu a)^{4-n} \frac{2^{6-2n}\pi}{2(n-1)\Gamma^2[\frac{1}{2}(n-1)]} \frac{\pi}{\sin\pi(n/2-2)} \frac{\pi}{\sin\pi(n-4)} A\left(-\frac{n}{2},-\frac{n}{2},-\frac{1}{2}(n-1)+Y\right)$$

$$\times \frac{\Gamma[\frac{1}{2}(n-1)-Y]\Gamma[\frac{1}{2}(n-1)+Y]}{\Gamma[2-\frac{1}{2}(n-1)-Y]\Gamma[2-\frac{1}{2}(n-1)+Y]} , \tag{25}$$

and expanding about $n = 4$ leads to

$$\Gamma^2_{Sf}[0] = \frac{g_t^2 N_f}{384\pi^2}\zeta^2 \left\{ \left(\frac{2}{\varepsilon}\right)^2 + [\tfrac{17}{3} - 3\gamma + \ln 4\pi\mu^2 a^2 - 2\psi(\tfrac{3}{2} - \sqrt{\tfrac{1}{4}-\zeta}) - 2\psi(\tfrac{3}{2} + \sqrt{\tfrac{1}{4}-\zeta})]\left(\frac{2}{\varepsilon}\right) \right\} . \tag{26}$$

Now we must include the counterterm $\delta\zeta_{g_t}$ in order to compensate the fermion loop in the boson propagator. This gives

$$\Gamma^2_{ctg_t}[0] = \frac{1}{2a^2}\delta\zeta_{g_t} \int d\sigma \, G_\zeta(\eta,\eta)$$

$$= \frac{1}{2\Gamma(n)}\delta\zeta_{g_t} \frac{\pi}{\sin\pi(n/2-2)} \frac{\Gamma[\frac{1}{2}(n-1)-Y]\Gamma[\frac{1}{2}(n-1)+Y]}{\Gamma[\frac{1}{2}+Y]\Gamma[\frac{1}{2}-Y]}$$

$$= \frac{g_t^2 N_f}{384\pi^2}\zeta^2 \left\{ -2\left(\frac{2}{\varepsilon}\right)^2 + \left[-\tfrac{22}{3} + 4\gamma + 2\psi(\tfrac{3}{2} - \sqrt{\tfrac{1}{4}-\zeta}) + 2\psi(\tfrac{3}{2} + \sqrt{\tfrac{1}{4}-\zeta}) \right]\left(\frac{2}{\varepsilon}\right) \right\} . \tag{27}$$

Combining Eqs. (26) and (27) gives

$$\Gamma_a^2[0] = \frac{g_t^2 N_f}{384\pi^2}\zeta^2\left\{-\left(\frac{2}{\varepsilon}\right)^2 + [-\tfrac{5}{3} + \gamma + \ln 4\pi\mu^2 a^2]\left(\frac{2}{\varepsilon}\right)\right\} , \tag{28}$$

which is canceled by the new counterterm

$$I_{\rm cta} = \int d\sigma\,\mu^{-\varepsilon}\frac{1}{a^4\Omega_5}\frac{g_t^2 N_f}{384\pi^2}\zeta^2\left[\left(\frac{2}{\varepsilon}\right)^2 - \left(\frac{2}{\varepsilon}\right)\right] . \tag{29}$$

Note that the nonlocal logarithmic term is canceled in the effective action by performing the integration and expanding the result about $n = 4$.

The scalar self-interaction, figure-eight diagram is simple to evaluate, with the result

$$\Gamma_{SS}^2[0] = \frac{\lambda}{768\pi^2}\zeta^2\left\{\left(\frac{2}{\varepsilon}\right)^2 + \left[\tfrac{14}{3} - 3\gamma + \ln 4\pi\mu^2 a^2 - 2\psi(\tfrac{3}{2} - \sqrt{\tfrac{1}{4} - \zeta}) - 2\psi(\tfrac{3}{2} + \sqrt{\tfrac{1}{4} - \zeta})\right]\left(\frac{2}{\varepsilon}\right)\right\} \tag{30}$$

and the associated counterterm

$$\Gamma_{\rm ct\lambda}^2[0] = \frac{1}{2a^2}\delta\zeta_\lambda\int d\sigma\, G_\zeta(\eta,\eta)$$

$$= \frac{\lambda}{768\pi^2}\zeta^2\left\{-2\left(\frac{2}{\varepsilon}\right)^2 + [-\tfrac{22}{3} + 4\gamma + 2\psi(\tfrac{3}{2} - \sqrt{\tfrac{1}{4} - \zeta}) + 2\psi(\tfrac{3}{2} + \sqrt{\tfrac{1}{4} - \zeta})]\left(\frac{2}{\varepsilon}\right)\right\} , \tag{31}$$

which combine to give

$$\Gamma_b^2[0] = \frac{\lambda}{768\pi^2}\zeta^2\left\{-\left(\frac{2}{\varepsilon}\right)^2\right.$$

$$\left. +[-\tfrac{8}{3} + \gamma + \ln 4\pi\mu^2 a^2]\left(\frac{2}{\varepsilon}\right)\right\} . \tag{32}$$

This divergence is canceled by the counterterm

$$I_{\rm ctb} = \int d\sigma\,\mu^{-\varepsilon}\frac{1}{a^4\Omega_5}\frac{\lambda}{768\pi^2}\zeta^2\left(\frac{2}{\varepsilon}\right)^2 . \tag{33}$$

It is important to note that for a conformal scalar field $\zeta=0$, there would be no divergence for the diagrams in Fig. 3.

C. Renormalization group equations

From Eqs. (12) to (16), we are able to derive the one-loop renormalization group equations for this model. We define

$$g_{t0} = \mu^{\varepsilon/2}Z_{g_t}Z_\phi^{-1/2}Z_2^{-1}g_t , \tag{34}$$

$$\lambda_0 = \mu^\varepsilon Z_\lambda Z_\phi^{-2}\lambda , \tag{35}$$

$$\zeta_0 = \zeta + \delta\zeta , \tag{36}$$

and given the non-Abelian coupling satisfies the flat space form

$$\mu\frac{\partial g}{\partial\mu} = -\left(\frac{\varepsilon}{2}\right)g - \frac{g^3}{16\pi^2}(\tfrac{11}{3}C_{\rm adj} - \tfrac{4}{3}T_f) , \tag{37}$$

differentiating the bare parameters with respect to μ, and setting the results to zero leads to

$$\mu\frac{\partial g_t}{\partial\mu} = -\left(\frac{\varepsilon}{2}\right)g_t + \frac{g_t}{16\pi^2}(g_t^2[N_f + \tfrac{3}{2}] - 6g^2 C_f) , \tag{38}$$

$$\mu\frac{\partial\lambda}{\partial\mu} = -\varepsilon\lambda + \frac{\lambda}{16\pi^2}(3\lambda + 4g_t^2 N_f) - \frac{12}{16\pi^2}g_t^4 N_f , \tag{39}$$

$$\mu\frac{\partial\zeta}{\partial\mu} = \frac{\zeta}{16\pi^2}(\lambda + 2g_t^2 N_f) . \tag{40}$$

Defining the bare gravitational parameter

$$D_6 = \mu^{-\varepsilon}\left\{D + (\tfrac{1}{24}\zeta^2 - \tfrac{1}{180})\left(\frac{2}{\varepsilon}\right) - \tfrac{11}{180}N_f\left(\frac{2}{\varepsilon}\right)\right.$$

$$\left. + \frac{g_t^2 N_f}{384\pi^2}\zeta^2\left[\left(\frac{2}{\varepsilon}\right)^2 - \left(\frac{2}{\varepsilon}\right)\right] + \frac{\lambda}{768\pi^2}\zeta^2\left(\frac{2}{\varepsilon}\right)^2\right\} \tag{41}$$

gives, after differentiating,

$$\mu\frac{\partial D}{\partial\mu} = \varepsilon D + (\tfrac{1}{12}\zeta^2 - \tfrac{1}{90}) - \tfrac{11}{90}N_f - \frac{g_t^2 N_f}{96\pi^2}\zeta^2 . \tag{42}$$

It is interesting that λ does not directly affect the running of D since there is no λ dependent single pole term in D_0. However, it influences indirectly through the running of ζ.

Specializing to one top quark coupled to SU(3) with n_q quarks contributing to the running of g, we have $C_f = \tfrac{8}{6}$, $N_f=3$, $C_{\rm adj} = 3$, and $T_f = \tfrac{1}{2}n_q$. Equations (37)–(42) become, at $n = 4$,

$$\mu \frac{\partial g}{\partial \mu} = -\frac{g^3}{16\pi^2}(11 - \tfrac{2}{3}n_q) , \qquad (43)$$

$$\mu \frac{\partial g_t}{\partial \mu} = \frac{g_t}{16\pi^2}(\tfrac{9}{2}g_t^2 - 8g^2) , \qquad (44)$$

$$\mu \frac{\partial \lambda}{\partial \mu} = \frac{\lambda}{16\pi^2}(3\lambda + 12g_t^2) - \frac{36}{16\pi^2}g_t^4 , \qquad (45)$$

$$\mu \frac{\partial \zeta}{\partial \mu} = \frac{\zeta}{16\pi^2}(\lambda + 6g_t^2) , \qquad (46)$$

$$\mu \frac{\partial D}{\partial \mu} = (\tfrac{1}{12}\zeta^2 - \tfrac{1}{90}) - \tfrac{33}{90} - \frac{g_t^2}{32\pi^2}\zeta^2 . \qquad (47)$$

D. Analysis

In this section we will numerically solve the renormalization group equations (43)–(47) from the wormhole scale, which is taken to $M_{\mathrm{wh}} = 10^{19}$ GeV, down to $\mu=1$ GeV. We take, in what follows, $n_q = 6$ and the strong coupling constant g to be $g_0=0.5$ at the wormhole scale. This choice gives $\alpha_s = g^2/4\pi \approx 1/7$ at 100 GeV, which is consistent with the value used in Ref. [15].

Putting the gravitational aspect aside for a moment, a short explanation of how the Yukawa and λ couplings determine the respective masses of the top quark and the Higgs boson is required. Note that the procedure here is the reverse of the procedure followed in Refs. [12,13] and is closer to the work of Ref. [15]. That is, we choose values of the bare couplings at the wormhole scale and evolve them down to the weak scale. In the standard model, the Higgs field acquires a vacuum expectation value, which can be calculated from the Fermi constant G_F, which we take to be $v \approx 245$ GeV. The mass of the top quark is then given by $m_t = (v/\sqrt{2})g_t$ and the physical Higgs boson $m_H^2 = \sqrt{-2\mu_H^2 - \tfrac{1}{a^2}\zeta} = (v^2/6)\lambda$, where $-\mu_H^2$ is the negative squared mass of the unbroken field. In the limit of large a, the effect of the zeta term is expected to be small. We also have the self-consistency condition that the couplings stop running when the mass scale of the respective particles is reached. This means that we must solve the equation $\mu = (v/\sqrt{2})g_t(\mu)$ for the top mass and $\mu^2 = (v^2/6)\lambda(\mu)$ for the Higgs boson mass. Figure 4 shows the top mass solution for a variety of initial values of g_{t0}. Note that as g_{t0} tends to large values, the top mass tends to a maximum value described as an "intermediate fixed point" by Hill [15]. Although the Yukawa coupling rises without limit at small values of $\ln\mu$ as a result of the strong coupling g, this is unphysical as the threshold condition marks the end of the running.

For the case of the Higgs boson mass, we have a more complicated situation. For large values of g_{t0}, the g_t^4 term dominates the running of λ for small λ_0 and the g_t^2 dominates for larger λ_0. The net result is that $\lambda(\mu)$ is pulled to another intermediate-type fixed point largely determined
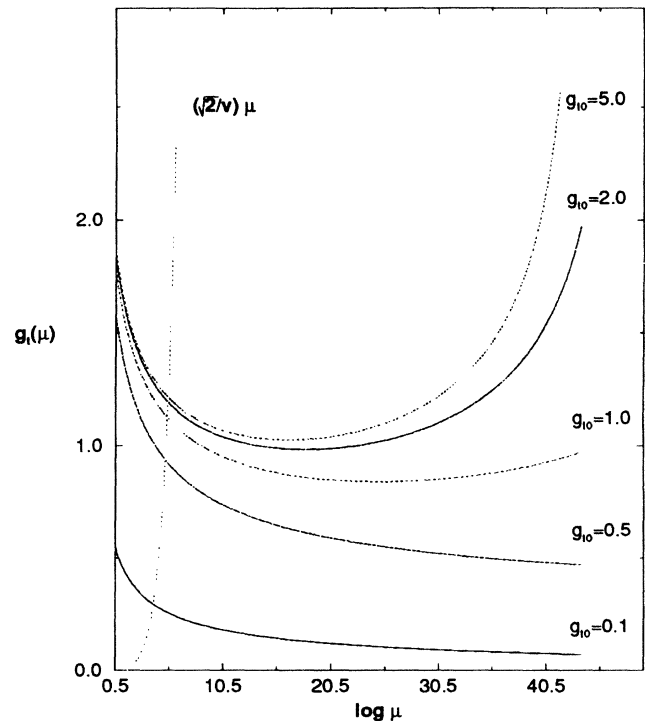

FIG. 4. $g_t(\mu)$ vs $\log\mu$. Here log represents the natural logarithm.

by the value of g_{t0}. This is essentially the merging of the upper and lower bounds described by Cabibbo et al. [12]. In Fig. 5, a series of curves is shown for various initial values λ_0 for $g_{t0}=2$ corresponding to a top mass $m_t=212$ GeV and a Higgs boson mass $m_H=158$ GeV. For smaller values of g_{t0}, the value of λ_0 becomes much more important. Figure 6 shows the behavior for $g_{t0}=0.2$, that is, $m_t=98$ GeV, again for a range of values of λ_0.

The general procedure for minimization of D is as follows. Given a value of ζ_0, one chooses the pair (g_{t0}, λ_0) and evolves the set of coupled renormalization group equations (43)–(47) down to the weak scale. The mass consistency equations are then solved to give the top quark and Higgs boson masses for the given pair of bare couplings. Now the terms in (47) will drop out at m_t for the fermion contribution and at m_H for the scalar contribution. The interaction term will drop out at whichever scale is reached first. Various threshold effects will also modify the total set of renormalization group equations as one or both particles drop out. Since we are assuming $\ln m_t$ and $\ln m_H$ are of a similar magnitude, we ignore such corrections in the following. Similarly, we will take as an approximation that half of the interaction term drops out at m_t and the other half at m_H. That is, we define the two quantities D_t and D_H such that $D = D_t + D_H$. The linearity of Eq. (47) then gives

$$\mu \frac{\partial D_t}{\partial \mu} = -\frac{33}{90} - \frac{g_t^2}{64\pi^2}\zeta^2 , \qquad (48)$$

$$\mu \frac{\partial D_H}{\partial \mu} = (\tfrac{1}{12}\zeta^2 - \tfrac{1}{90}) - \frac{g_t^2}{64\pi^2}\zeta^2 . \qquad (49)$$
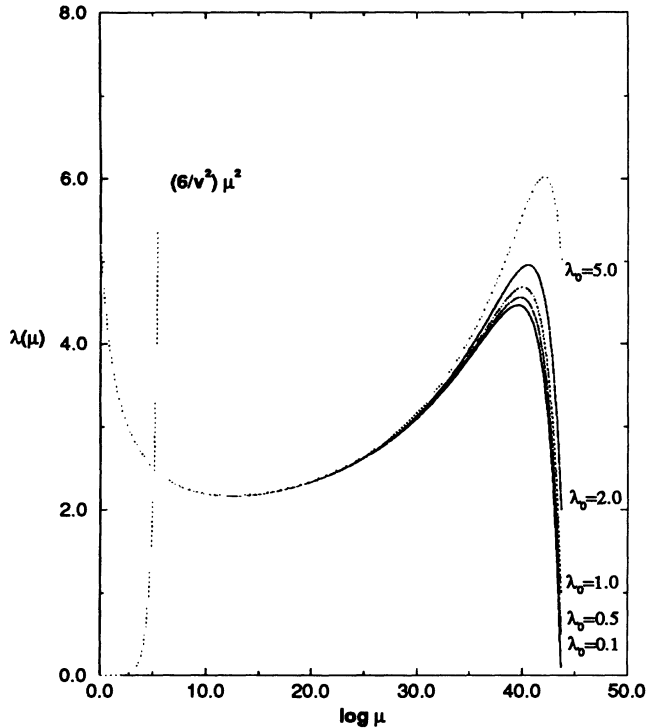
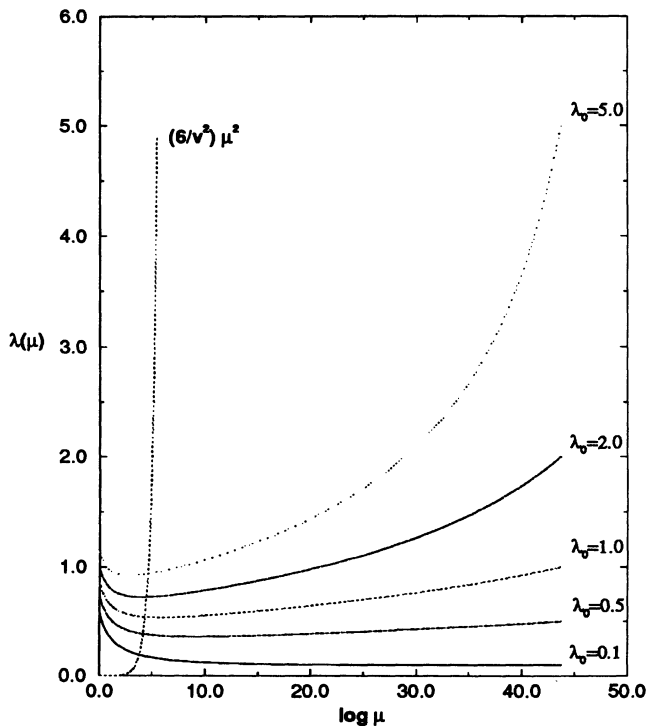FIG. 5. $\lambda(\mu)$ vs $\log\mu$, for g_{t0}=2.0. Here log represents the natural logarithm.

FIG. 6. $\lambda(\mu)$ vs $\log\mu$, for g_{t0}=0.2. Here log represents the natural logarithm.

We then evaluate $D_t(m_t)$ and $D_H(m_H)$. Since this is the end of the running for each quantity, the results may be combined to give $D_{\text{final}} \equiv D_t(m_t) + D_H(m_H)$. It is this quantity D_{final} which must be minimized. This quantity may be evaluated for a range of values (g_{t0}, λ_0), for a given ζ_0, and if D_{final} assumes an absolute minimum for a particular pair of couplings, then the conclusion will be that wormholes force the couplings, and hence the masses, to these precise values. The procedure may be repeated for different ζ_0 to see the effect on the predicted masses.

A brief discussion of the consistency of the above procedure is necessary. We have given no explanation as to why the Higgs vacuum expectation value (VEV) is $v \approx 245$ GeV. This is fixed by the negative, unbroken, mass-squared parameter μ_H^2. Now, in the spherical formalism, all the previous calculations go through unchanged if we include a mass term for the Higgs boson, provided we make the substitution $\zeta \to \zeta + \mu_H^2 a^2$. This will then require the introduction of counterterms which renormalize the cosmological constant Λ and Newton's constant G. Presumably, on dimensional grounds, the minimization of these parameters will fix the mass of the scalar. However, we make no attempt to describe how this may occur. Therefore it may appear as if our attempt to predict the mass of the scalar is inconsistent. However, a short argument will convince the reader that this is not so. Given our particular choice of $v \approx 245$ GeV, we may find a set of bare couplings $\zeta_0, g_{t0}, \lambda_0, \ldots$ such that D_{final} is minimized. This will give us a prediction of the masses and, therefore, μ_H^2 at the weak scale. If we choose a different value v' for the Higgs VEV, then we will find a different set of couplings $\zeta_0', g_{t0}', \lambda_0', \ldots$ and hence a difference $\mu_H'^2$. Consistency then implies that if we have $\mu_H'^2$ as the value fixed by minimizing Λ and G, then we would have a VEV of v'. We assume, therefore, that there is a one-to-one correspondence between $\langle\phi\rangle = v$ and $\mu_H(m_H)$ at the minimization point. Given that experiment tells us that $v \approx 245$ GeV, we uniquely evaluate the fixed, but unknown μ_H^2.

E. Results

Before presenting the results a few preliminary observations can be made.

First, as far as D is concerned, the sign of ζ is irrelevant, since ζ=0 is a fixed point of Eq. (46) and all quantities depend on ζ^2.

For ζ=0, the sign of the one-loop coefficient in D_H is negative, and so D_{final} will be minimized for large values of m_t and m_H. This leads to the prediction that the top mass will be pulled to its largest possible value consistent with unitarity, an observation first made by Grinstein and Hill [5]. The Higgs boson mass will also get pulled up to its largest value, determined by the merging of the upper and lower bounds with respect to m_t, as described in Ref. [12], as a result of domination by the large value of g_t. In the framework of this simple model, we obtain the previously mentioned values m_t=216 GeV and m_H=163 GeV. This behavior is expected for nonzero ζ provided

$\zeta_0 \ll \sqrt{\frac{2}{15}}$, the critical value in Eq. (49).

For large $\zeta_0 \gg 1$, $\zeta(\mu)$ remains large over the full evolution even for reasonably large $g_{t0} \geq 1$. This implies that $D_H(m_H)$ is minimized for the smallest possible value of m_H. For large ζ_0, $D_H(m_H)$ is minimized for by choosing small λ_0 and small g_{t0}, as both must be small in order for m_H to be minimized. $D_H(m_H)$ will overcome the disadvantage of a small top mass in $D_t(m_t)$ provided $(\frac{1}{12}\zeta^2 - \frac{1}{90}) \gg \frac{33}{90}$. However, one must assume that the dependence of ζ_0 on the wormhole $\{\alpha_i\}$ parameters prevents the value from increasing without bound, since $D_H(m_H)$ can be made arbitrarily small for sufficiently large ζ_0. Also, one must remember that for small g_{t0} the electroweak couplings will become important and may act to put a lower limit on the Higgs boson mass through the requirement that $\langle\phi\rangle = v$ remain the absolute minimum of the potential. Such limits were given by Linde [11] and Weinberg [10].

We turn now to the numerical results. Figures 7–12 show the value of D_{final} for $0.001 < g_{t0} < 2.0$ and $0.001 < \lambda_0 < 1.0$ over a range of values of ζ_0 from 0.1 to 10.0. However, one should bear in mind that the approximation of neglecting the electroweak couplings probably means that for $g_{t0} \leq 0.1$ the procedure is invalid. Also, although a maximum value of $\lambda_0 = 1.0$ is rather low given the perturbative limit $\lambda \approx 50$, given our definitions, the behavior for large values of λ_0 is essentially flat and uninteresting.

First, for $\zeta_0 = 0.1$ we see in Fig. 7 the expected preference for large values of g_{t0}. There is a surprise, however, that even in this limit, where λ is expected to have little effect, the minimum of D_{final} occurs along the line $\lambda_0 = 0.001$, which is effectively zero with respect to g_t. Now as ζ_0 is increased to $\zeta_0 = 0.3$, the"potential" D_{final} exhibits a kink at about $g_{t0} = 0.5$ and begins to increase again. This is extremely interesting as we have a definite minimum value of D_{final} and so a preferred value of m_t. Note again that the minimum occurs again along the line $\lambda_0 = 0.001$. This behavior continues as ζ_0 is increased further, with the link becoming more pronounced and moving farther toward the lower end of the range of g_{t0}. As we get to very large values of ζ_0, the kink disappears
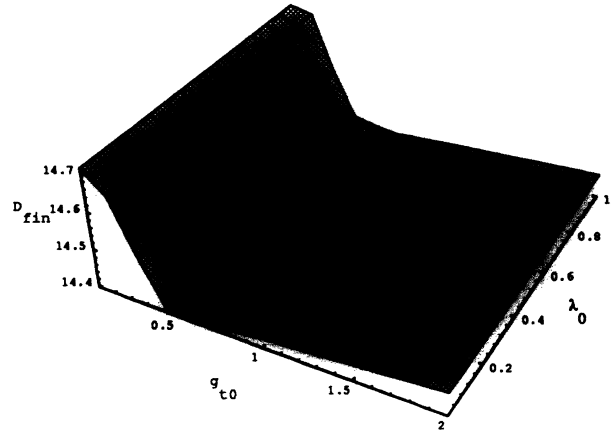

FIG. 8. D_{final} vs (λ_0, g_{t0}), for $\zeta_0 = 0.3$.
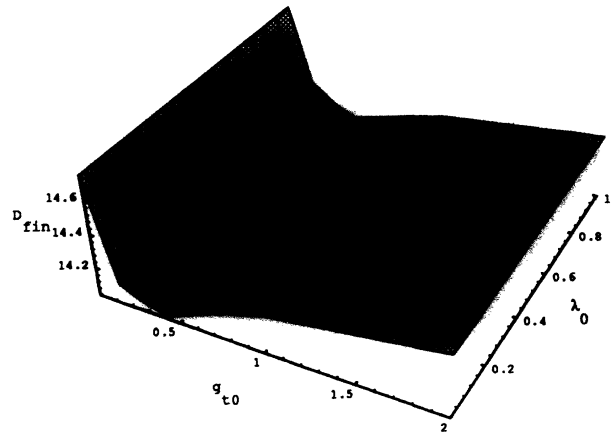
FIG. 9. D_{final} vs (λ_0, g_{t0}), for $\zeta_0 = 0.5$.
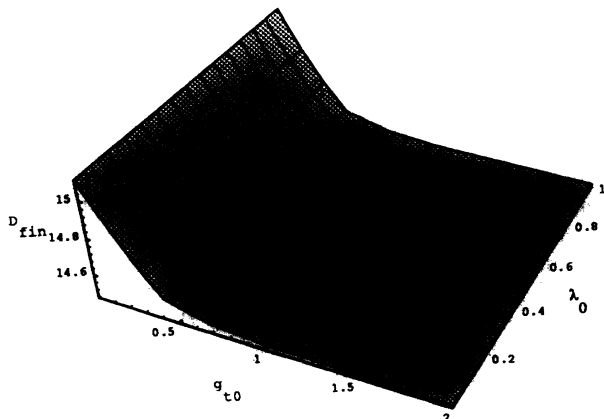
FIG. 7. D_{final} vs (λ_0, g_{t0}), for $\zeta_0 = 0.1$.
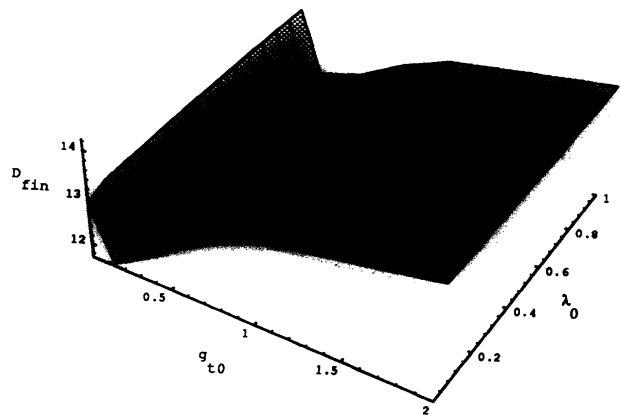
FIG. 10. D_{final} vs (λ_0, g_{t0}), for $\zeta_0 = 1.0$.
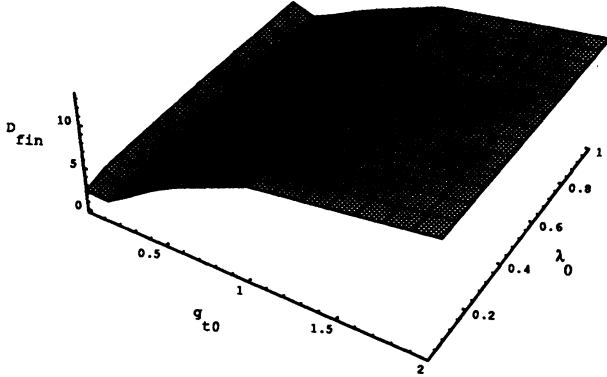
FIG. 11. D_{final} vs (λ_0, g_{t0}), for $\zeta_0 = 2.0$.

and we tend to the limit of small couplings, as we expect.

Looking at the behavior of the potential D_{final} for intermediate values of ζ_0, we have the expected repulsion away from small g_{t0} due to the coefficient $-\frac{33}{90}$ in Eq. (48). Now, as we raise the value of g_{t0}, this begins to cause $\zeta(\mu)$ to run down at a faster rate. This has the effect of decreasing the rate at which $D_H(\mu)$ runs down, and if ζ_0 runs down to below $\sqrt{\frac{2}{15}}$, $D_H(\mu)$ in fact begins to rise with decreasing scale. Therefore a point is reached where one loses more by running $\zeta(\mu)$ down than the gain of raising m_t. This explains the kink in the potential. Clearly, the relative strength of the respective forces changes with the initial value ζ_0. For small ζ_0, maximizing m_t will win out, but for large ζ_0 it will be much easier to slow the running of $\zeta(\mu)$ by lowering the couplings. For the case of λ_0, it appears that it is always more efficient to slow the running of $\zeta(\mu)$ than to raise or lower λ_0 to move the Higgs boson mass depending on whether the one-loop coefficient in Eq. (49) is positive or negative. This is probably due to the fact that m_H depends on $\sqrt{\lambda}$ rather than the linear relationship between g_t and m_t. It also appears that the interaction term in Eq. (42) plays little part compared to the running of ζ.

Therefore the minimization hypothesis unambiguously predicts the following. First, for a given value of ζ_0 the masses of the top quark and the Higgs boson are uniquely
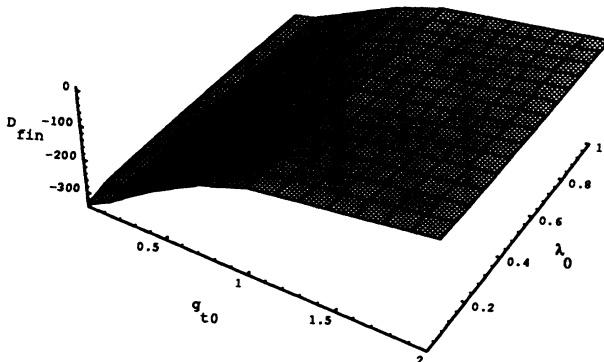
FIG. 12. D_{final} vs (λ_0, g_{t0}), for $\zeta_0 = 10.0$.

determined. A range of values of m_t and m_H is given in Table I. We also list for future reference the quantity $\Delta \equiv \zeta^2(m_H) - \frac{2}{15}$, which is proportional to the one-loop coefficient in Eq. (49) and as such is a measure of the Higgs boson contribution to the conformal anomaly [19]. Second, and perhaps more importantly, given that the ζ_0 parameter is unknown, we nevertheless predict that the Higgs boson mass is forced to the lowest possible value with respect to the top mass. This is the constraint that the Higgs potential remain bounded below up to the wormhole scale and corresponds to the lower bound given in Ref. [12] and improved upon in a review by Sher [16]. Given the improving statistics on the possible top mass [17], we can predict a range of values where the Higgs boson mass is likely to lie. In our simple model, the possible top masses fall between about $\zeta_0 = 0.4$ and 0.6. This leads to the bounds 40 GeV $< m_H <$ 80 GeV. This bound is most likely to be too low as a result of electroweak corrections. Simply applying the lower-bound prediction to the lower bound given in [16], we predict that the top mass is most likely to be 60 GeV $< m_H <$ 130 GeV. This appears to be more realistic.

As a final remark, in the absence of any constraint on ζ_0, if we make the totally ad hoc assumption that the Higgs field conformal anomaly vanishes at m_H, so that m_H will fall at the minimum of $D_H(\mu)$ as a function of μ, then there is only one value of ζ_0 which satisfies this constraint. We find, to the accuracy of this analysis, $\zeta_0 = 0.493 \pm 0.001$, which corresponds to $m_t = 126.2 \pm 0.3$ GeV and $m_H = 59.1 \pm 0.3$ GeV. Allowing for an increase of 10% or so for m_t and perhaps a little more for m_H because of electroweak corrections, this value is highly consistent with the current experimental data fits. While we do not claim to have uniquely predicted the top and Higgs boson masses, this appears to be an extremely interesting coincidence.

IV. DISCUSSION

In this paper, we have investigated, using the techniques of previous papers [7,8,20] the consequences of the Coleman wormhole hypothesis for the couplings and masses of the standard model. We looked at the effect of vacuum diagrams up to two-loop order on the renormalization of the higher-order curvature terms in Eq. (20). When projected onto a four-sphere, we have the parameter $D \equiv \frac{8\pi}{3} d$, where d is a combination of the higher-

TABLE I. Top and Higgs boson masses for various ζ_0.

ζ_0	g_{t0}	m_t (GeV)	m_H (GeV)	Δ
10.0	0.012	9	3.2	99.638
2.0	0.035	23	3.7	3.807
1.0	0.107	60	14	0.762
0.6	0.225	107	43	0.108
0.5	0.283	125	58	0.006
0.4	0.373	147	80	−0.069
0.3	0.549	173	110	−0.115
0.1	no min	216	163	−1.333

order couplings in Eq. (2), which must be minimized in the infrared limit.

Using a model incorporating a nonconformally coupled Higgs scalar, we derived the renormalization group equations for the matter couplings, the nonconformal coupling ζ, and the gravitational parameter D. We then proceeded to investigate whether or not D developed a minimum for various values of the bare top quark Yukawa coupling g_{t0} and the bare Higgs self-coupling λ_0 given a fixed value of ζ_0. We found that for all values of ζ_0, D is minimized for the smallest possible value of λ_0, leading to the prediction that the Higgs boson mass is pushed to its lowest possible value relative to the top mass. Also, D develops a minimum for a particular value of g_{t0}, provided that ζ_0 is in an intermediate range. For large ζ_0 the top mass is pushed to a low value, and for small ζ_0 it

is pushed to a large value. Using the current experimental predictions for the mass of the top quark, we were able to give a possible range for the mass of the Higgs boson. Also, assuming that the conformal anomaly for the Higgs field vanishes at the scale of the Higgs boson mass, we obtained a unique prediction for m_t and m_H which is consistent with current bounds.

APPENDIX A: FEYNMAN RULES FOR NONCONFORMAL SCALARS

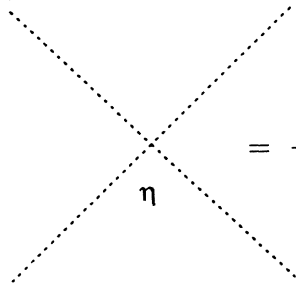The propagator of a nonconformal scalar field is

$$
G_\zeta(\eta_1, \eta_2) = a^2 \sum_{l=0}^{\infty} \frac{1}{[l + \frac{1}{2}(n-1) + Y][l + \frac{1}{2}(n-1) - Y]} Y_{lm}(\eta_1) Y_l^{*m}(\eta_2)
$$

$$
\equiv a^2 \sum_{l=0}^{\infty} G_\zeta(l) Y_{lm}(\eta_1) Y_l^{*m}(\eta_2)
$$

$$
\equiv \quad 1 \quad\quad\quad 2 \tag{A1}
$$

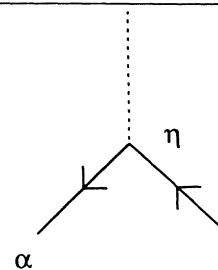
with

$$
Y = \sqrt{\tfrac{1}{4} - \zeta^2} . \tag{A2}
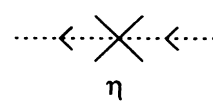$$

The interaction rules are
(1) Self coupling:

$$
= -\lambda \tag{A3}
$$

(2) Yukawa coupling (top quark):

$$
= -\frac{g_t}{\sqrt{2}} \delta^\alpha{}_\beta . \tag{A4}
$$

(3) Conformal counterterm:

$$
= -\frac{1}{a^2} \delta\zeta . \tag{A5}
$$

[1] S. Coleman, Nucl. Phys. **B307**, 867 (1988).
[2] S. Coleman, Nucl. Phys. **B310**, 643 (1988).
[3] G. M. Shore, Phys. Rev. D **21**, 2226 (1980).
[4] B. Grinstein and M. Wise, Phys. Lett. B **212**, 407 (1988).
[5] B. Grinstein and C. T. Hill, Phys. Lett. B **220**, 520 (1989).
[6] G. M. Shore, Ann. Phys. (N.Y.) **117**, 121 (1979).
[7] B. A. Harris and G. C. Joshi, Int. J. Mod. Phys. (to be published).
[8] B. A. Harris and G. C. Joshi, Class. Quantum Grav. (to be published).
[9] B. H. Lee and H. Nishino, Phys. Lett. B **234**, 473 (1990).
[10] S. Weinberg, Phys. Rev. Lett. **36**, 294 (1976).
[11] A. D. Linde, JETP Lett. **23**, 64 (1976).
[12] N. Cabibbo, L. Maiani, G. Parisi, and R. Petronzio, Nucl. Phys. **B170**, 480 (1980).
[13] T. D. Cheng, E. Eichen, and L. F. Li, Phys. Rev. D **9**, 2259 (1974).
[14] B. Pendelton and G. G. Ross, Phys. Lett. **98B**, 291 (1981).
[15] C. T. Hill, Phys. Rev. D **24**, 691 (1981).
[16] M. Sher, Phys. Rep. **179**, 273 (1989).
[17] F. del Aguila, M. Martinez, and M. Quiros, Nucl. Phys. **B381**, 451 (1992).
[18] C. Itzykson and J. B. Zuber, *Quantum Field Theory* (McGraw-Hill, New York, 1985).
[19] N. D. Birrell and P. C. W. Davies, *Quantum Fields in Curved Space* (Cambridge University Press, Cambridge, England, 1982).
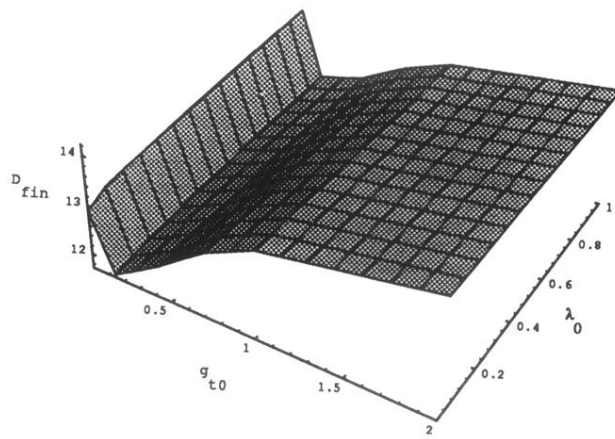[20] B. A. Harris and G. C. Joshi, Int. J. Mod. Phys. A **9**, 3245 (1994).

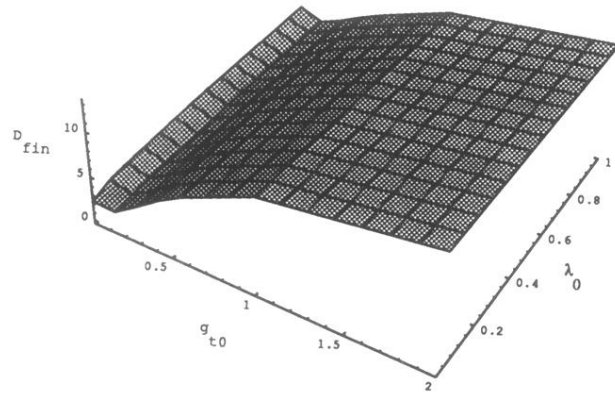FIG. 10. D_{final} vs (λ_0, g_{t0}), for $\zeta_0 = 1.0$.

FIG. 11. D_{final} vs (λ_0, g_{t0}), for $\zeta_0 = 2.0$.
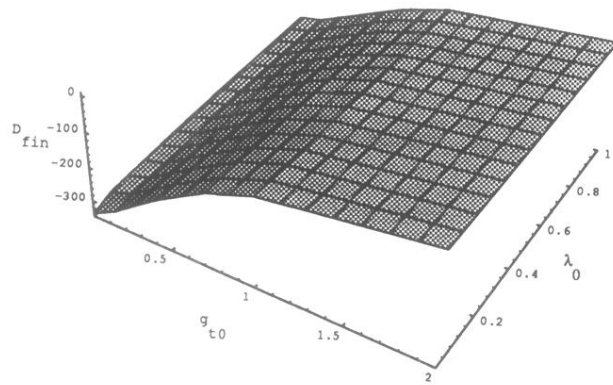
FIG. 12. D_{final} vs (λ_0, g_{t0}), for $\zeta_0=10.0$.
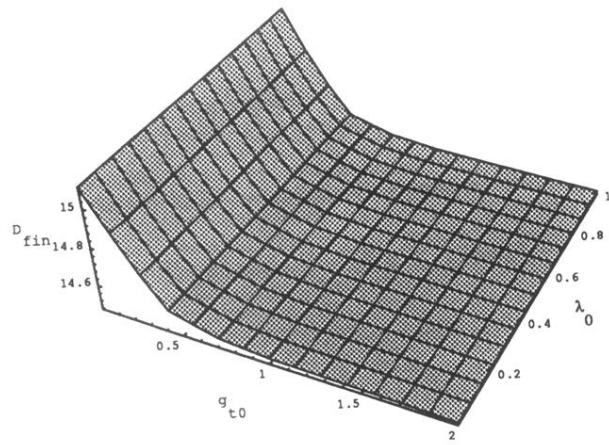
FIG. 7. D_{final} vs (λ_0, g_{t0}), for $\zeta_0 = 0.1$.

FIG. 8. D_{final} vs (λ_0, g_{t0}), for $\zeta_0 = 0.3$.

FIG. 9. D_{final} vs (λ_0, g_{t0}), for $\zeta_0 = 0.5$.